

Spin-wave dispersion in half-doped  $\text{La}_{3/2}\text{Sr}_{1/2}\text{NiO}_4$ D. X. Yao<sup>1</sup> and E. W. Carlson<sup>2</sup><sup>1</sup>*Department of Physics, Boston University, Boston, Massachusetts 02215, USA*<sup>2</sup>*Department of Physics, Purdue University, West Lafayette, Indiana 47907, USA*

(Received 12 September 2006; revised manuscript received 28 November 2006; published 30 January 2007)

Recent neutron scattering measurements reveal spin and charge ordering in the half-doped nickelate,  $\text{La}_{3/2}\text{Sr}_{1/2}\text{NiO}_4$ . Many of the features of the magnetic excitations have been explained in terms of the spin waves of diagonal stripes with a magnetic coupling structure which is fourfold symmetric. However, an optical mode dispersing away from the  $(\pi, \pi)$  point was not captured by this theory. We show here that this apparent optical mode is a natural consequence of stripe twinning in a diagonal stripe pattern with a magnetic coupling structure which is twofold symmetric, i.e., one possessing the same spatial rotational symmetry as the ground state.

DOI: [10.1103/PhysRevB.75.012414](https://doi.org/10.1103/PhysRevB.75.012414)

PACS number(s): 75.30.Ds, 75.10.Hk, 71.27.+a

The strong electronic correlations in many novel materials often lead to spontaneous electronic inhomogeneity at the nanoscale. Evidence of these possibly new phases, with local modulations in the charge or spin degrees of freedom, has been seen in many experimental probes, such as NMR,  $\mu\text{SR}$ , STM, and neutron scattering.<sup>1-3</sup> In the cuprate high temperature superconductors and the related nickelate compounds, neutron scattering has proven especially useful for identifying the underlying patterns, especially when there is an ordered component to the spins. Spin wave theory in particular has been remarkably good at predicting the magnetic excitations of static spin order in these systems.<sup>4-9</sup> Recent neutron scattering experiments show universal behavior in the high energy magnetic excitation spectra of three types of cuprate superconductors (YBCO, LSCO, and LSCO).<sup>2</sup> We are interested here in the high energy magnetic excitations of the related nickelate compounds, since the low energy scattering spectra are similar to the cuprates, yet without superconductivity.

Recent experiments on doped  $\text{La}_{2-x}\text{Sr}_x\text{NiO}_4$  have shown clear evidence of static diagonal charge and spin stripe order.<sup>10,11</sup> We consider here the experiments by Freeman *et al.* on the spin dynamics of half-doped  $\text{La}_{3/2}\text{Sr}_{1/2}\text{NiO}_4$  using inelastic neutron scattering.<sup>9</sup> In this material, the spins are in a diagonal stripe phase, where stripes run  $45^\circ$  from the Ni-O bond direction, and the charged domain walls are only two lattice constants apart.

Spin wave theory has been successful at describing much of the behavior in spin-ordered nickelates.<sup>4-9</sup> In Ref. 9, many features of the neutron scattering data of  $\text{La}_{3/2}\text{Sr}_{1/2}\text{NiO}_4$  were captured using spin wave theory based on a fourfold symmetric spin coupling pattern [i.e., that of Fig. 1(a) with  $J_c = J_d = 0$ ]. However, there was an extra magnetic mode observed to disperse away from the antiferromagnetic wave vector  $Q_{\text{AF}} = (0.5, 0.5)$  above 50 meV in Fig. 3 of Ref. 9 which was not captured. One suggestion put forth by the authors is that diagonal discommensurations in the spin order may be able to account for this extra scattering mode. We show here that the mode could also be due to a twofold symmetric pattern in the spin coupling constants (i.e., with  $J_c \neq J_d$ ). In this case the “extra mode” is really an extension of the acoustic band, made visible due to stripe twinning.

The observed ordering vector is  $Q = (0.275, 0.275)$ , which

is close to a commensurate stripe value of  $Q = (0.25, 0.25)$ . The slight deviation from commensurability is believed to be due to the discommensurations described above. Since we are interested in describing relatively high energy effects, in what follows we neglect the small incommensurability, and consider commensurate diagonal stripe structures of spacing  $p=2$ . We consider two patterns in this paper: Site-centered stripes as shown in Fig. 1(a), and the corresponding bond-centered stripes shown in Fig. 1(b).

To model these two systems, we use a suitably parametrized Heisenberg model on a square lattice,

$$H = \frac{1}{2} \sum_{i,j} J_{i,j} \mathbf{S}_i \cdot \mathbf{S}_j, \quad (1)$$

where the indices  $i$  and  $j$  run over all sites, and the couplings  $J_{i,j}$  are illustrated in Fig. 1. For diagonal, site-centered stripes of spacing  $p=2$  (DS2), there is no need for nearest-neighbor coupling, and so we set  $J_a = 0$ . The straight-line coupling  $J_b$  across the domain wall is antiferromagnetic. The diagonal coupling  $J_c$  across the domain wall is also antiferromagnetic, but the diagonal coupling  $J_d$  parallel to the stripes we take to be ferromagnetic,  $J_d < 0$ , as explained below. In the diagonal bond-centered case (DB2), the nearest neighbor coupling  $J_a > 0$  is finite and antiferromagnetic. We also include the ferromagnetic coupling  $J_b < 0$  across the domain wall. Since we are interested in describing high energy effects, we neglect the very weak single-ion anisotropy term, which splits the twofold degenerate acoustic band at low energy.

The model considered in Ref. 9 is that of site-centered stripes [Fig. 1(a)] with  $J_c = J_d = 0$ . In that case, the spin system reduces to two interpenetrating antiferromagnets, with two separate Néel vectors but identical Néel ordering temperatures. Any finite diagonal coupling ( $J_c \neq 0$  or  $J_d \neq 0$ ) is sufficient to establish a unique relative direction between the two Néel vectors, and the ground state becomes the stripe structure shown in Fig. 1(a). The number of reciprocal lattice vectors is also decreased by a factor of 2 in the presence of the diagonal couplings  $J_c \neq 0$  or  $J_d \neq 0$ , as can be seen in the Bragg peaks of Figs. 1(c) and 1(d) and in the spin wave dispersion relations of Fig. 2. In both cases, independent of the value of  $J_c$  and  $J_d$ , although the antiferromagnetic point  $Q_{\text{AF}}$  is a magnetic reciprocal lattice vector and therefore must

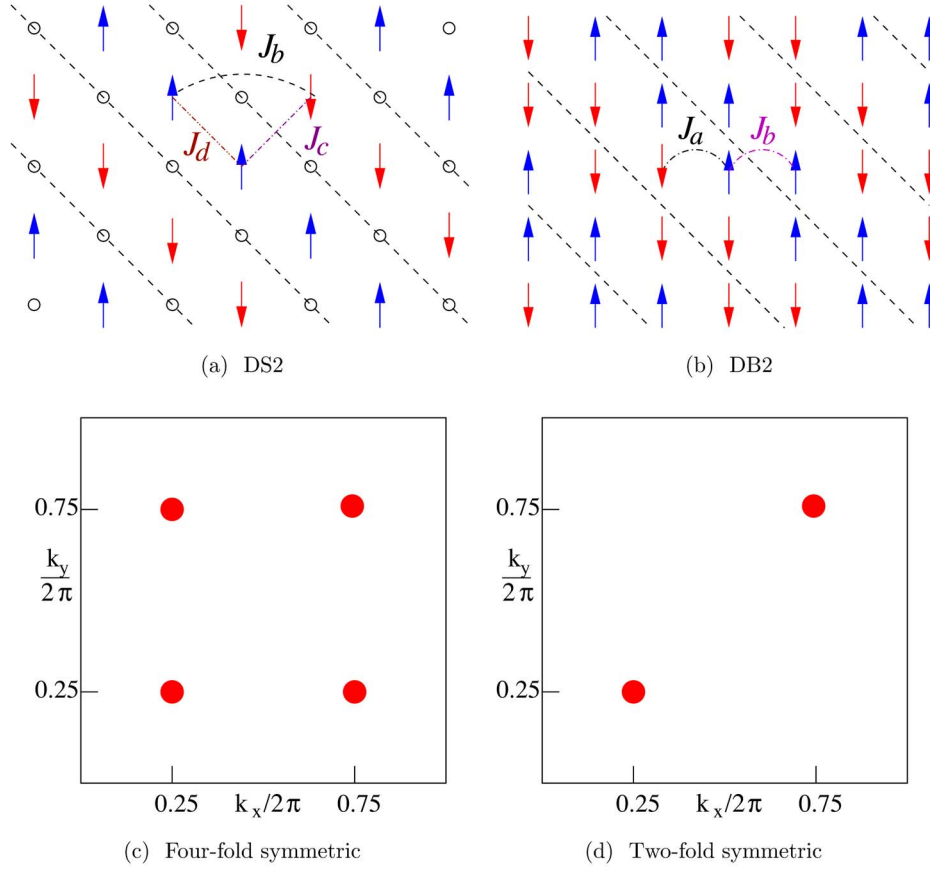


FIG. 1. (Color online) Spin-charge ordering in a  $\text{NiO}_2$  square lattice. Arrows represent spins on  $\text{Ni}^{2+}$  sites and circles represent  $\text{Ni}^{3+}$  holes. (a) DS2: Diagonal, site-centered stripes of spacing  $p=2$ . The straight-line exchange coupling across the charge domain wall is  $J_b$ , and  $J_c$  and  $J_d$  are diagonal couplings perpendicular and parallel to the charge domain wall, respectively. (b) DB2: Diagonal, bond-centered stripes of spacing  $p=2$ . The nearest neighbor antiferromagnetic coupling is  $J_a$ , and  $J_b$  is the ferromagnetic coupling across domain walls. (c) When  $J_c = J_d = 0$  for DS2, the magnetic Bragg peaks are fourfold symmetric. (d) When  $J_c \neq J_d$  for DS2, and for any coupling pattern for DB2, the magnetic Bragg peaks are twofold symmetric.

have a spin wave cone dispersing out of it, there is no net antiferromagnetism in the system, so that weight is forbidden at zero frequency at  $Q_{\text{AF}}$ .

Another key feature of nonzero couplings  $J_c$  and  $J_d$  for site-centered stripes is the symmetry of the spin wave structure, as shown in Fig. 2. In the limit where  $J_c = J_d = 0$ , the spin wave dispersion is symmetric under  $90^\circ$  rotations, as shown in Fig. 2(a). However, when either  $J_c$  or  $J_d$  or both are nonzero, the symmetry is broken, and the spin wave structure is now only symmetric under  $180^\circ$  rotations, as shown in Fig. 2(b). This means that for any nonzero  $J_c$  or  $J_d$ , the spin wave velocity of the acoustic mode dispersing out of  $Q_{\text{AF}} = (0.5, 0.5)$  is different parallel and perpendicular to the stripe direction. In the presence of stripe twins, the two velocities will appear as two branches in plots of  $\omega$  vs.  $\vec{k}$ , as shown in Fig. 3.

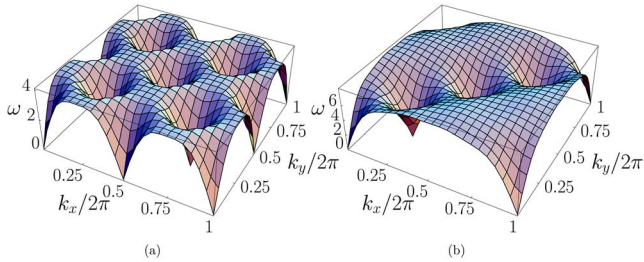


FIG. 2. (Color online) Spin wave dispersion relations of diagonal site-centered stripes (DS2). (a)  $J_c = J_d = 0$ ; (b)  $J_c = J_b$ ,  $J_d = -0.5J_b$ . The energy  $E$  is in units of  $J_b S$ .

The magnon dispersion from Eq. (1) can be solved analytically for DS2,

$$\omega(k_x, k_y) = 2\sqrt{A^2 - B^2}, \quad (2)$$

where

$$A = 2J_b + J_c - J_d + J_d \cos(k_x - k_y),$$

$$B = J_b \cos(2k_x) + J_b \cos(2k_y) + J_c \cos(k_x + k_y). \quad (3)$$

There are two different spin wave velocities for the cones emanating from the IC peak  $Q_{\text{IC}} = (0.25, 0.25)$  and symmetry-related points, one corresponding to spin wave velocities perpendicular to the direction of the domain walls (i.e., perpendicular to the stripes), and the other parallel to the direction of the domain walls,

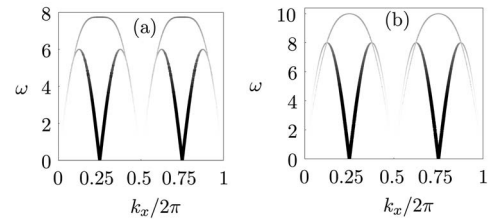


FIG. 3. DS2: Diagonal, site-centered stripes of spacing  $p=2$ . The plots are for twinned stripes, summing contributions along  $(k_x, k_x)$  and  $(k_x, -k_x)$ . (a)  $J_c = J_b$  and  $J_d = -0.5J_b$ ; (b)  $J_c = 2J_b$  and  $J_d = -0.5J_b$ . The energy  $E$  is in units of  $J_b S$ .

$$v_{\perp} = 4(2J_b + J_c),$$

$$v_{\parallel} = 4\sqrt{(2J_b + J_c)(2J_b - J_d)}. \quad (4)$$

In Fig. 3, we show the expected dispersions and scattering intensities for DS2. Plots are shown for twinned stripes, summing the contributions parallel and perpendicular to the stripe direction, i.e., along the  $(k_x, -k_x)$  and  $(k_x, k_x)$  directions, respectively. Because  $J_c$  and  $J_d$  are nonzero, there is an apparent optical mode. Note that it is not a true optical mode, since in this configuration there are only two spins per unit cell, leading to only one (twofold degenerate) band. As in the bond-centered case, weight is forbidden at low energy at the antiferromagnetic point  $Q_{AF}$ , so that the spin-wave cone emanating from this magnetic reciprocal lattice vector has vanishing weight as  $\omega \rightarrow 0$ . In Fig. 3(a), we have set  $J_c = J_b$  and  $J_d = -0.5J_b$ . In Fig. 3(b), we use  $J_c = 2J_b$  with  $J_d = -0.5J_b$ . Notice that in panel (a) of the figure, the apparent optical mode is flat.

We have chosen the coupling constants with the following in mind: The “acoustic” branch peaks at  $\omega(3\pi/4, 3\pi/4) = 4J_b + 2J_c$ . The apparent “optical” mode peaks at  $\omega(\pi/2, 3\pi/2) = 4\sqrt{(2J_b - J_d)(J_c - J_d)}$ . The data indicate that the apparent optical mode is higher in energy than the top of the “acoustic” part:  $\omega(\pi/2, 3\pi/2) > \omega(3\pi/4, 3\pi/4)$ , which implies that

$$J_d \leq (1/2)(2 + J_c - \sqrt{2}\sqrt{4 + J_c^2}) \quad (5)$$

when  $J_b = 1$ . However, the extra mode above 50 meV is not too high in energy, so parameters need to be chosen so as to satisfy this constraint, but remain close to the equality.

We also require the apparent “optical” branch to be concave, since there is no evidence of a dip in the extra mode. This requirement gives

$$\frac{\partial^2}{\partial k_x^2} \omega(k_x, -k_x) = \frac{4(J_d - 2)(J_c - 2 - 2J_d)}{\sqrt{-(J_c - J_d)(J_d - 2)}} \leq 0, \quad (6)$$

resulting in the constraint that

$$J_d \leq \frac{1}{2}J_c - 1. \quad (7)$$

As long as the second constraint, Eq. (7), is satisfied in the range  $0 \leq J_c \leq 2J_b$ , then the first constraint, Eq. (5), is also satisfied. To describe the data, then, we find that we need a sizeable  $J_c$ , on the order of  $J_b$ . This makes  $J_c$  significantly larger than that reported at the lower doping  $x = 1/3$ , where diagonal site-centered stripes of spacing  $p = 3$  (DS3) were used to explain the data successfully.<sup>11</sup> Although the fits in Ref. 11 were good for  $J_c = 0$  and were not significantly improved by letting  $J_c$  increase to  $J_c \approx 0.5J_b$ , the data were still well described using a nonzero  $J_c$ . We find that the data at doping  $x = 1/3$  are also well described by taking  $J_c$  to be as large as  $J_b$  or even  $2J_b$  as in our Fig. 3.

We also find that we need  $J_d < 0$ , i.e., the diagonal coupling parallel to the stripes needs to be ferromagnetic, in order to describe the data. If one considers the diagonal spin couplings  $J_c$  and  $J_d$  to be derived from, e.g., a perturbative treatment of a single-band Hubbard or three-band Emery

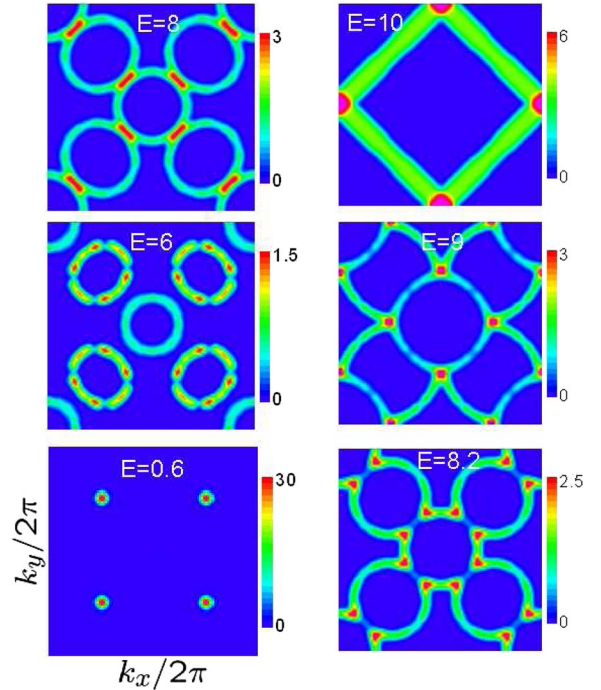


FIG. 4. (Color online) Constant energy cuts with windows of  $0.1J_bS$  for twinned diagonal, site-centered stripes of spacing  $p=2$  at  $J_c=2J_b$  and  $J_d=-0.5J_b$ . The energy  $E$  is in units of  $J_bS$ .

model on a square Ni-O lattice, we expect  $J_c = J_d$ . Given that the spin ground state breaks the fourfold rotational symmetry of the square lattice to only twofold rotational symmetry, any finite spin-lattice coupling results in the two diagonal directions being inequivalent, and leads to  $J_c \neq J_d$ . For weak rotational symmetry breaking of the square lattice in the perturbative regime, one expects  $J_c = J_o + \epsilon$  with  $J_d = J_o - \epsilon$  where  $\epsilon$  is small compared to  $J_o$ , so that the anisotropy between the two diagonal coupling directions is weak as well. [This preserves the spin ground state of Fig. 1(a).] We find, however, that this regime of the coupling constants leads to the apparent optical mode being too low in energy to capture the data. This may indicate that the materials are far from the perturbative limit of the single-band Hubbard or three-band Emery model.

Figure 4 shows constant energy cuts for DS2 corresponding to the parameters in Fig. 3(b). An important feature of this configuration is that although the antiferromagnetic point  $Q_{AF} = (0.5, 0.5)$  is a magnetic reciprocal lattice vector, zero-frequency weight is forbidden there by symmetry, since the stripes have no net Néel vector at  $Q_{AF}$ . Combined with the fact that there is no optical band, this means that the DS2 configuration *can never have spectral weight at the antiferromagnetic point  $Q_{AF}$* , even at finite frequency. Notice that as energy is increased in Fig. 4, a faint spin wave cone emerges from  $Q_{AF}$  in a light ring of scattering, but none of the constant energy plots show any weight at  $Q_{AF}$ . This is consistent with the constant energy plots for  $\text{La}_{3/2}\text{Sr}_{1/2}\text{NiO}_4$  shown in Ref. 9. By contrast, the corresponding bond-centered configuration (DB2) shown in Fig. 1(b) has an optical band which displays a saddlepoint at  $Q_{AF}$ , and rather large scattering intensity at finite frequency at  $Q_{AF}$  as a result. (See

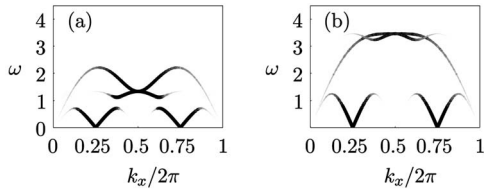


FIG. 5. DB2: Diagonal, bond-centered stripes of spacing  $p=2$ . [See Fig. 1(b).] The plots are for twinned stripes, summing contributions along  $(k_x, k_x)$  and  $(k_x, -k_x)$ . (a) Very weak coupling across the domain wall, with  $J_b = -0.1J_a$ . (b) Weak coupling across the domain wall, with  $J_b = -0.5J_a$ . The energy  $E$  is in units of  $J_a S$ .

Fig. 5 of this paper, as well as Fig. 8 of our previous paper, Ref. 5.)

While we find that diagonal, site-centered stripes of spacing  $p=2$  (DS2) with twofold symmetric couplings are able to account for the behavior of the apparent optical mode observed to disperse away from  $Q_{AF}$  in Fig. 3 of Freeman *et al.*,<sup>9</sup> there are two other high energy features which our model has not captured. One is the asymmetry in intensity observed above 30 meV in the spin wave cones emanating from the main IC peaks. The other is a mode in the 31–39 meV range propagating away from  $(h, k)$  structural reciprocal lattice points. These (as well as the apparent optical mode) have been attributed to discommensurations in the magnetic order.<sup>9</sup>

Although site-centered stripes can explain the “extra” mode, we find that bond-centered stripes cannot. In Fig. 5, we show the expected dispersions and intensities for the diagonal, *bond-centered* stripes (DB2) shown in Fig. 1(b). This configuration has a true optical mode. Figure 5(a) shows weak coupling across the charged domain walls, with  $J_b = -0.1J_a$ , and Fig. 5(b) has somewhat stronger coupling across the domain walls, with  $J_b = -0.5J_a$ . Note that in the bond-centered case, couplings across the domain walls are ferromagnetic. Results are shown for twinned stripe patterns, summing the contribution parallel and perpendicular to the stripe direction, i.e., along the  $(k_x, -k_x)$  and  $(k_x, k_x)$  directions, respectively. Although there is a reciprocal lattice vector at  $Q_{AF}$ , weight is forbidden there at zero frequency, since the Néel vector switches sign across the domain walls. We have reported the analytic form of the spin wave dispersion in this case in a previous publication.<sup>4</sup>

Because this spin configuration is only  $180^\circ$  symmetric,

the spin-wave velocity emanating from  $Q_{AF}$  is different parallel and perpendicular to the stripe direction. However, the branch emanating from  $Q_{AF}$  in the direction parallel to stripes has so little weight as to be effectively invisible in the plots. This configuration displays a true optical mode because there are four spins in the unit cell. The optical mode has a *saddlepoint* at  $Q_{AF}$  and finite energy, with increased weight at the saddlepoint. For weak coupling across the domain walls ( $|J_b| < |J_a|$ ), the optical mode always displays significant weight at  $Q_{AF}$  at finite frequency. This is not supported by the data,<sup>9</sup> which at the energies measured display no scattering at  $Q_{AF}$  and finite frequency. This likely indicates that the domain walls are not bond-centered in this material, but are probably site-centered.

In conclusion, we have used linear spin-wave theory to describe the magnetic excitations recently observed in neutron scattering<sup>9</sup> on  $\text{La}_{3/2}\text{Sr}_{1/2}\text{NiO}_4$ . Many features of the data were captured in the spin wave analysis of Ref. 9. Other features, including an apparent optical mode dispersing away from  $Q_{AF}$  above 50 meV, were attributed to discommensurations in the spin order. We show here that the apparent optical mode may also be captured in linear spin wave theory by using a spin coupling configuration that preserves the symmetry of the spin ground state. Namely, we have shown that diagonal, site-centered stripes of spacing  $p=2$  capture this mode when the pattern of couplings is twofold symmetric, rather than fourfold symmetric. This is because the twofold symmetric coupling pattern gives rise to two different spin-wave velocities (i.e.,  $v_{\parallel} \neq v_{\perp}$ ) emanating from the antiferromagnetic point  $Q_{AF} = (0.5, 0.5)$ . For twinned samples, the two velocities are simultaneously visible, and the higher velocity mode  $v_{\parallel}$  parallel to the stripes is responsible for the “extra” scattering above 50 meV. Furthermore, this configuration is forbidden to display scattering at the antiferromagnetic point  $Q_{AF}$  at any energy, whereas bond-centered stripes have a true optical mode with significant weight at  $Q_{AF}$ , which is not supported by the data. We therefore conclude that the magnetic excitations observed in Ref. 9 are consistent with site-centered stripes, but not with bond-centered stripes.

It is a pleasure to thank D. K. Campbell and A. T. Boothroyd for helpful discussions. This work was supported by Boston University (D.X.Y.), and by the Purdue Research Foundation (E.W.C.). E.W.C. is a Cottrell Scholar of Research Corporation.

<sup>1</sup>For a review, see, e.g., E. W. Carlson, V. J. Emery, S. A. Kivelson, and D. Orgad, in *The Physics of Superconductors*, Vol. II, edited by J. Ketterson and K. Benneman (Springer-Verlag, Berlin, 2004), and references therein.

<sup>2</sup>J. M. Tranquada, cond-mat/0512115.

<sup>3</sup>E. Dagotto, *Science* **309**, 257 (2005).

<sup>4</sup>E. W. Carlson, D. X. Yao, and D. K. Campbell, *Phys. Rev. B* **70**, 064505 (2004).

<sup>5</sup>D. X. Yao, E. W. Carlson, and D. K. Campbell, *Phys. Rev. B* **73**, 224525 (2006).

<sup>6</sup>J. M. Tranquada, P. M. Gehring, G. Shirane, S. Shamoto, and M. Sato, *Phys. Rev. B* **46**, 5561 (1992).

<sup>7</sup>P. Bourges, Y. Sidis, M. Braden, K. Nakajima, and J. M. Tranquada, *Phys. Rev. Lett.* **90**, 147202 (2003).

<sup>8</sup>F. Krüger and S. Scheidl, *Phys. Rev. B* **67**, 134512 (2003).

<sup>9</sup>P. G. Freeman, A. T. Boothroyd, D. Prabhakaran, C. Frost, M. Enderle, and A. Hiess, *Phys. Rev. B* **71**, 174412 (2005).

<sup>10</sup>A. T. Boothroyd, D. Prabhakaran, P. G. Freeman, S. J. S. Lister, M. Enderle, A. Hiess, and J. Kulda, *Phys. Rev. B* **67**, 100407(R) (2003).

<sup>11</sup>H. Woo, A. T. Boothroyd, K. Nakajima, T. G. Perring, C. Frost, P. G. Freeman, D. Prabhakaran, K. Yamada, and J. M. Tranquada, *Phys. Rev. B* **72**, 064437 (2005).